applied sciences

MDPI

Article

Reconfigurable Terahertz Metamaterial Using Split-Ring Meta-Atoms with Multifunctional Electromagnetic Characteristics

Yuhang Liao and Yu-Sheng Lin *

State Key Laboratory of Optoelectronic Materials and Technologies, School of Electronics and Information Technology, Sun Yat-Sen University, Guangzhou 510275, China; liaoyh9@mail2.sysu.edu.cn

* Correspondence: linyoush@mail.sysu.edu.cn; Tel.: +86-188-0205-4660

Received: 1 July 2020; Accepted: 29 July 2020; Published: 30 July 2020

Abstract: We propose a reconfigurable terahertz (THz) metamaterial (RTM) to investigate its multifunctional electromagnetic characteristics by moving the meta-atoms of split-ring resonator (SRR) array. It shows the preferable and capable adjustability in the THz frequency range. The electromagnetic characteristics of the proposed RTM device are compared and analyzed by moving the meta-atoms in different polarized transverse magnetic (TM) and transverse electric (TE) modes. The symmetrical meta-atoms of RTM device exhibit a resonant tuning range of several tens of GHz and the asymmetrical meta-atoms of RTM device exhibit the better tunability. Therefore, an RTM device with reconfigurable meta-atoms possesses the resonance shifting, polarization switching, electromagnetically induced transparency (EIT) switching and multiband to single-band switching characteristics. This proposed RTM device provides the potential possibilities for the use of THz-wave optoelectronics with tunable resonance, EIT analog and tunable multiresonance characteristics.

Keywords: metamaterial; terahertz; optical switching; electromagnetically induced transparency; resonator

1. Introduction

In the last two decades, there has been increasing interest in terahertz (THz) metamaterial optics spanning the spectrum range of 0.1 THz to 10 THz [1,2]. Metamaterials are not natural materials. It means that they are artificially designed [3] and engineered to span the whole electromagnetic spectrum, including visible [4–6], infrared [7–12], THz [13–23] and microwaves [24]. Metamaterials possess many extraordinary and useful optical properties such as negative refractive index [25], metalensing [26], cloaking [27] and perfect absorbance [28], etc. Many studies have reported about THz metamaterials being used in sensors, filters and absorbers [28–32]. Among these THz metamaterials, the split-ring resonator (SRR) is a simple plane structure that possesses unique electric and magnetic characteristics. Therefore, there have been many diversified metamaterials developed in the last few years [4–23], such as U-shaped SRR [33], three-dimensional (3D) SRRs [34], C-shaped SRRs [35], V-shaped SRRs [10], spiral-shaped SRRs [23] and H-shaped SRRs [36], etc.

The capability of actively tunable metamaterials plays an important role in exploring flexible and applicable electromagnetic characteristics [35–37]. There have been several methods reported to achieve tunable metamaterials. These include—but are not limited to—electrical and magnetic driving, optical pumping, thermal tuning and mechanical control [21–23]. Through these controllable methods, the geometric morphology of the metamaterials can be reconfigured by curling, rotating and reshaping the metamaterial unit cell. Therefore, we can control numerous electromagnetic properties of metamaterials actively, such as resonant frequency, electromagnetically induced transparency (EIT) analog and multiband switching [14–19].

In this study, we propose and investigate a reconfigurable THz metamaterial (RTM) with multifunctional electromagnetic characteristics by moving the meta-atoms of SRR array, which exhibits the active tunability in the THz frequency range. By moving the inner arrangement of the SRR array, the transmission spectra show the tunable resonances and the switchable EIT analog. This RTM design opens the door to the use of THz-wave optoelectronics in filters, polarizers, switches and sensor applications.

2. Design and Method

Figure 1a,b shows the schematic drawings of the proposed RTM device configured with four SRR meta-atoms and the geometrical denotations of the RTM unit cell, respectively. The thickness of the SRR meta-atoms is 300 nm on silicon on insulator (SOI) substrate. The permittivities of Au and Si materials are assumed as constants in this study. They are 10^4 for Au layer and 10 for Si substrate, respectively [37]. For a convenient description, we denote these four SRR meta-atoms as SRR-1, SRR-2, SRR-3 and SRR-4. The line width of each SRR meta-atom is 6 μm and the period of SRR array is 100×100 μm^2 ($P_x \times P_y$). The length (L) and width (W) of each SRR meta-atom are 30 μm. The distance between the SRR meta-atoms (G) is 2 μm. The coordinates of the incident electromagnetic wave in transverse electric (TE) and transverse magnetic (TM) modes are also illustrated in Figure 1a, where E, H and k are the electric field, magnetic field and wave vector of the incident electromagnetic wave, respectively. In this study, each SRR meta-atom is designed to move along the x- or y-axis direction and to investigate the corresponding electromagnetic responses. We define each SRR meta-atom that has its own reference position denoted as (x_i, y_i), where i is each SRR meta-atom, i.e., i = 1, 2, 3 and 4, as shown in Figure 1b. The center points of SRR meta-atoms are the initial reference positions whose variations represent the movement of each SRR meta-atom. The initial reference positions are $(x_1, y_1) = (-16, 16)$, $(x_2, y_2) = (16, 16)$, $(x_3, y_3) = (-16, -16)$ and $(x_4, y_4) = (16, -16)$, respectively. The electromagnetic characteristics of SRR array will be investigated by moving SRR meta-atoms to six different (x_2, x_4), (y_1, y_2), (y_2, y_4), x_2, (x_2, x_3) and (y_2, y_3) positions.

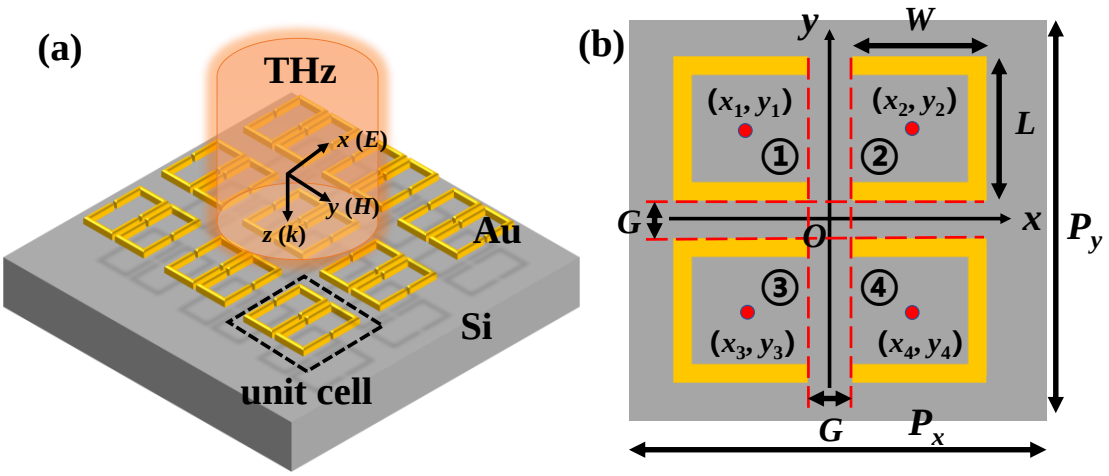

Figure 1. (**a**) Schematic drawing of the proposed reconfigurable terahertz (THz) metamaterial (RTM) device with four split-ring resonator (SRR) meta-atoms; (**b**) The geometric parameters of four SRR meta-atoms. The geometric dimensions are: W = 30 μm, L = 30 μm, G = 2 μm and $P_x = P_y$ = 100 μm. The reference points are $(x_1, y_1) = (-16, 16)$, $(x_2, y_2) = (16, 16)$, $(x_3, y_3) = (-16, -16)$ and $(x_4, y_4) = (16, -16)$.

In simulations, the incident electromagnetic wave is a plane wave, whose propagation direction is perpendicular to the x-y plane. The boundary conditions are set periodic for x-y plane and perfectly matched for the z plane. The electromagnetic filed monitor is set on the bottom of the substrate to

calculate the transmission of the incident THz wave. The resonances of the engineered SRR meta-atoms can be expressed by [13]

$$f_{LC} = \left(\frac{c_0}{2\pi P\sqrt{\varepsilon_s}}\right)\sqrt{\frac{G}{W}} \quad (1)$$

where c_0 represents the velocity of light in a vacuum, P is the period of SRR array (Px and Py in this study), ε_s is the relative permittivity of the materials in the SRR array, G is the gap width and W is the width of the SRR meta-atom.

3. Results and Discussions

Figure 2 presents the simulated transmission spectra of the RTM device obtained by moving the SRR-2 and SRR-4 meta-atoms along the positive x-axis direction in TE and TM modes. The values of y_2 and y_4 are kept at the initial positions. It has two resonances at 0.49 THz and 0.92 THz for the initial state (x_2, x_4) = (16, 16) in TE mode, which is shown as the black curve in Figure 2a. By moving the position of (x_2, x_4) from (16, 16) to (32, 32) along the positive x-axis direction in TE mode, the first resonance is blue-shifted from 0.49 THz to 0.54 THz. The tuning range is 50 GHz. The second resonance is blue-shifted from 0.92 THz to 0.96 THz with a tuning range of 40 GHz. In TM mode, there are three initial resonances at 0.50 THz, 0.67 THz and 0.91 THz as shown by the black curve in Figure 2b. The first resonance is slightly red-shifted from 0.50 THz to 0.48 THz, the second resonance is red-shifted from 0.67 THz to 0.65 THz, and the third resonance is red-shifted from 0.91 THz to 0.89 THz. These results indicate that the reconfigured SRR meta-atoms have minor THz tunability in TE and TM modes.

In order to investigate the influence of moving the SRR-1 and SRR-2 meta-atoms, the values of x_1 and x_2 are kept at the initial positions while y_1 and y_2 are changed. The simulated transmission spectra are obtained by moving the SRR-1 and SRR-2 meta-atoms along positive y-axis direction in TE and TM modes as shown in Figure 3a,b, respectively. In TE mode, there are two initial resonances at 0.49 THz and 0.92 THz. When (y_1, y_2) moves to (32, 32), the resonances are almost identical. It is because the TE-field coupling effect within the inner SRR meta-atoms has no change along x-axis direction. In TM mode, there are three resonances at 0.50 THz, 0.67 THz and 0.91 THz for the initial state of (y_1, y_2) = (16, 16). By moving the (y_1, y_2) position to above (20, 20), the first and third resonances vanish gradually, and the second resonance shifts to 0.72 THz for (y_1, y_2) = (32, 32). These properties are suitable for the metamaterial to be used in the tunable polarized multiresonance application.

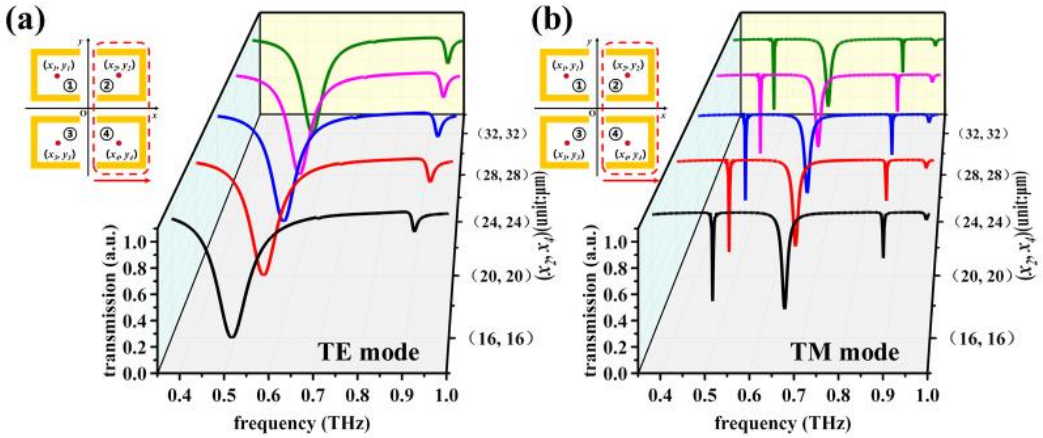

Figure 2. Simulated transmission spectra of the RTM device obtained by moving the SRR-2 and SRR-4 meta-atoms along the positive x-axis direction in (**a**) transverse electric (TE) and (**b**) transverse magnetic (TM) modes.

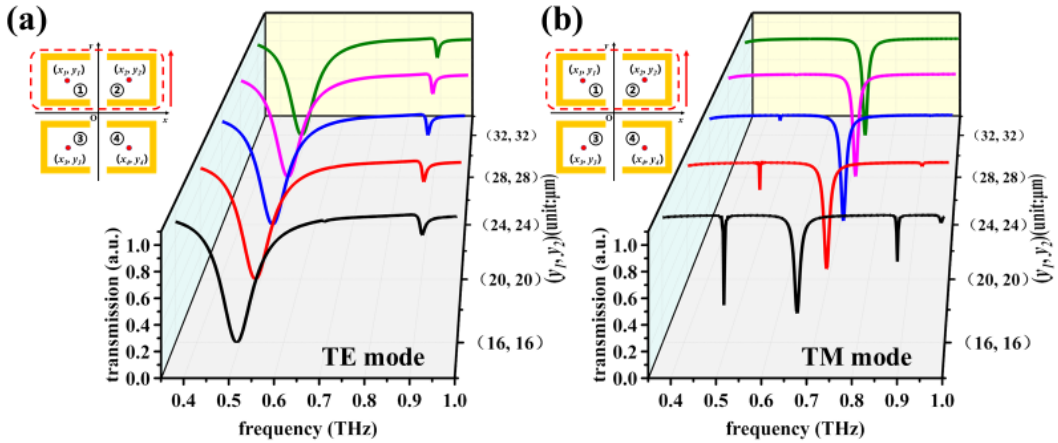

Figure 3. Simulated transmission spectra of the RTM device obtained by moving the SRR-1 and SRR-2 meta-atoms along positive y-axis direction in (**a**) TE and (**b**) TM modes.

Figure 4 shows the simulated transmission spectra of the RTM device obtained by moving the SRR-2 and SRR-4 meta-atoms along the positive y-axis direction in TE and TM modes. The x_2 and x_4 values are set to the initial positions, i.e., (16, 16). The y_2 and y_4 values are moved from 16 μm to 32 μm and from −16 μm to 0 μm, respectively. When the SRR-2 and SRR-4 meta-atoms are moved from the position (16, −16) to (20, −12), a sharp resonant peak at the first resonance appears, which is the bright-mode resonance in the EIT analog owing to the stronger electromagnetic coupling energy between the asymmetrical SRRs. In TE mode, there are two resonant modes of the RTM device, which are broadband resonance generated by the localized surface plasmons within SRR meta-atoms and the narrowband resonance produced by the surface diffraction wave from the periodic SRR array. When they are tuned to superimpose, these two resonances will couple together and then generate a Fano-resonance. Therefore, the RTM device exhibits the EIT analog characteristic. In order to understand the interactions between the THz wave and the SRR array, an electromagnetic field monitor is set in the SRR array. The corresponding electromagnetic field distributions are shown in Figure 5 to illustrate the electric field (E-field) and magnetic field (H-field), respectively. When the position of (y_2, y_4) changes continuously, the resonance is slightly blue-shifted with a tuning range of 20 GHz. Figure 4b shows the transmission spectra of the RTM device in TM mode. It is clear that the change has no remarkable influence on the resonances, which means that the RTM device has a stable performance by moving the SRR-2 and SRR-4 meta-atoms along the positive y-axis direction in TM mode.

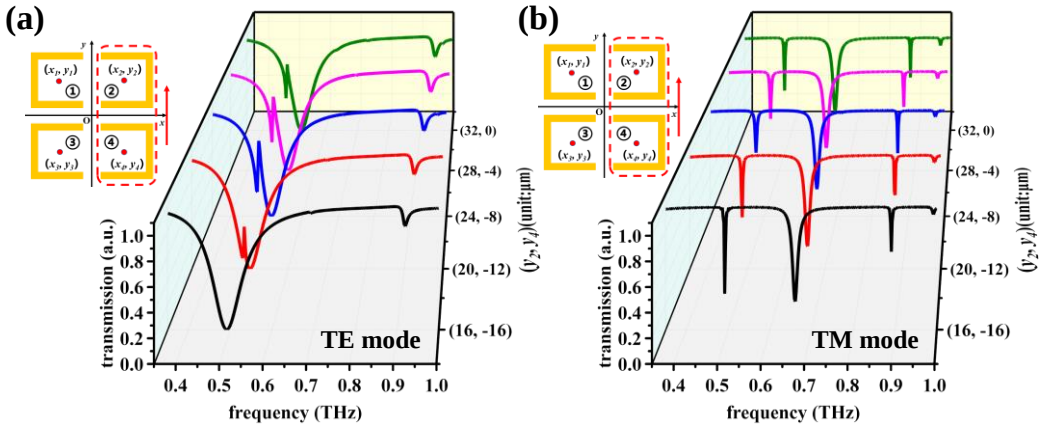

Figure 4. Simulated transmission spectra of the RTM device obtained by moving the SRR-2 and SRR-4 meta-atoms along positive y-axis direction in (**a**) TE and (**b**) TM modes.

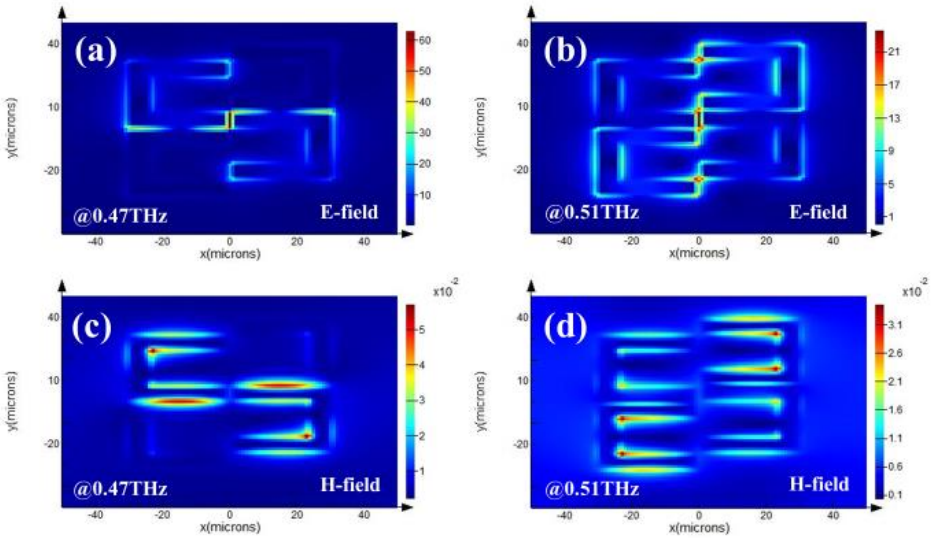

Figure 5. (**a**,**b**) E-field and (**c**,**d**) H-field distributions of the RTM device with (y_2, y_4) = (24, −8) μm in TE mode.

Figure 6a,b shows the simulated transmission spectra of RTM device by moving SRR-2 meta-atom along positive x-axis direction in TE and TM modes, respectively. In order to achieve a better understanding of the physical mechanism related to the electromagnetic response, the corresponding E-field and H-field distributions of SRR-2 meta-atom with x_2 = 24 μm in TE mode are shown in Figure 7. In TE mode, there is a resonance at 0.49 THz for the initial state of x_2 = 16 μm as shown in Figure 6a. When x_2 value moves to 20 μm, there is an additional EIT response found at 0.45 THz. When SRR-2 meta-atom continuously moves to 24 μm, 28 μm and 32 μm, there are two EIT resonances at 0.45 THz and 0.51 THz. There are nonuniform E-field distributions shown in Figure 7a–c. These unbalanced electromagnetic energies result in the generations of Fano resonances. In TM mode, there are three resonances at 0.50 THz, 0.67 THz and 0.91 THz as shown in Figure 6b. These three resonances are insensitive to the movement of SRR-2 meta-atom along positive x-axis direction. It indicates the proposed RTM device exhibits the tunable EIT resonance in TE mode and stable resonance in TM mode.

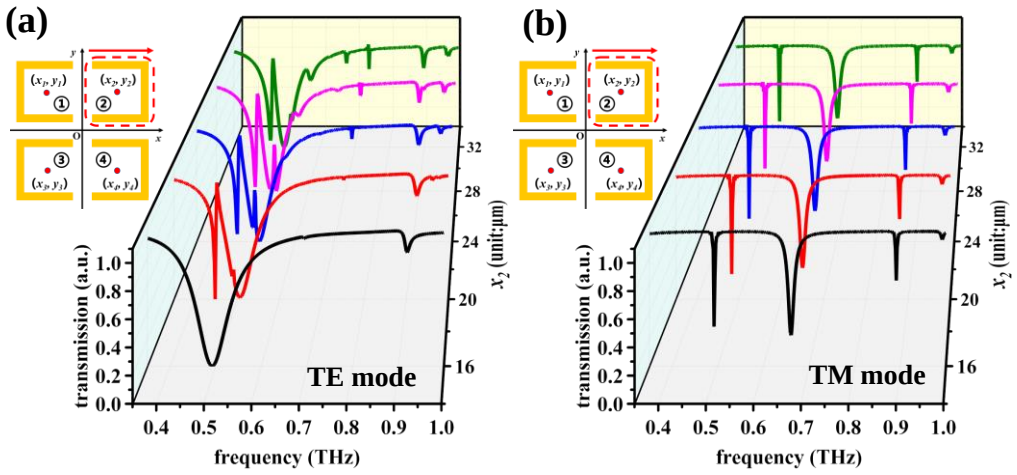

Figure 6. Simulated transmission spectra of the RTM device obtained by moving the SRR-2 meta-atom along positive x-axis direction in (**a**) TE and (**b**) TM modes.

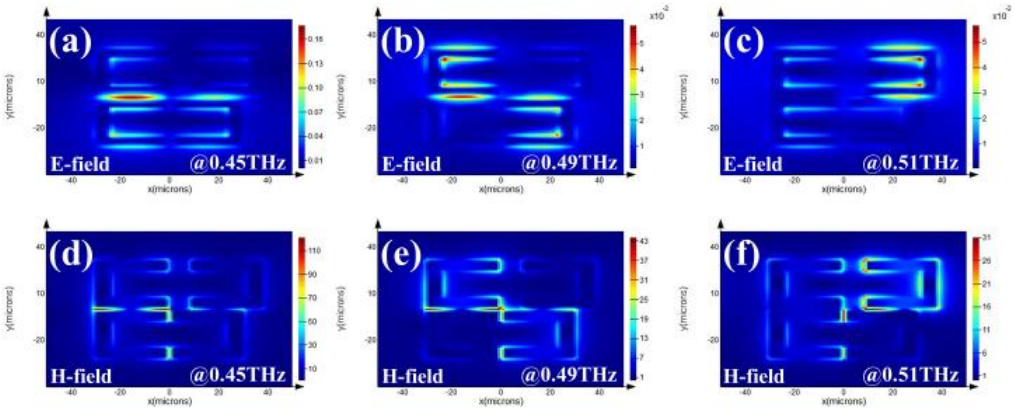

Figure 7. (**a**–**c**) E-field and (**d**–**f**) H-field distributions of the RTM device with x_2 = 24 μm in TE mode.

To control the electromagnetic response of the proposed RTM design, SRR-2 and SRR-3 meta-atoms are moved symmetrically along positive and negative x-axis directions. x_2 and x_3 values are moved from the position of (16, −16) to (32, −32), while y_2 and y_3 values are kept at the initial positions. Figure 8 shows the simulated transmission spectra of the RTM device by moving SRR-2 and SRR-3 meta-atoms along positive and negative x-axis directions in TE and TM modes, respectively. In TE mode, when the position of (x_2, x_3) moves from (16, −16) to (32, −32), the resonances are almost kept constant as shown in Figure 8a. In TM mode, there are three resonances at 0.50 THz, 0.67 THz and 0.91 THz for the initial state of (x_2, x_3) = (16, −16) as the black curve shown in Figure 8b. By moving x_2 and x_3 values symmetrically along both x-axis directions from the position of (16, −16) to (32, −32), the first and third resonances will vanish gradually while the second resonance is stable at 0.67 THz. Such RTM design provides the possibility of optical switch application.

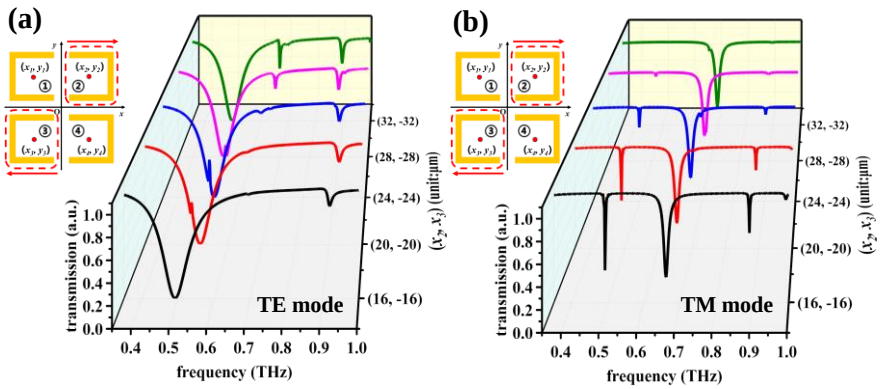

Figure 8. Simulated transmission spectra of the RTM device obtained by moving the SRR-2 and SRR-3 meta-atoms along positive and negative x-axis directions in (**a**) TE and (**b**) TM modes, respectively.

Figure 9 shows the simulated transmission spectra of the RTM device by moving SRR-2 and SRR-3 meta-atoms along positive and negative y-axis directions in TE and TM modes. In TE mode, there are two resonances found at 0.49 THz and 0.92 THz for the initial state of (y_2, y_3) = (16, −16) as shown in Figure 9a. By moving y_2 and y_3 values symmetrically along positive and negative y-axis directions, an additional EIT resonance appears at about 0.53 THz, while the one at 0.92 THz remains stable. In TM mode, there are three resonances at 0.50 THz, 0.67 THz and 0.91 THz for the initial state of (y_2, y_3) = (16, −16) as the black curve shown in Figure 9b. By moving y_2 and y_3 values symmetrically along positive and negative y-axis directions, the first and the third resonances vanish while the second resonance remains quite stable and constant. This means that these resonances can be switched from

triple-band to single-band resonance in TM mode. Therefore, this proposed SRRs can be used as an EIT switch in TE mode and multi-band to single-band switch in TM mode by changing y_2 and y_3 values symmetrically.

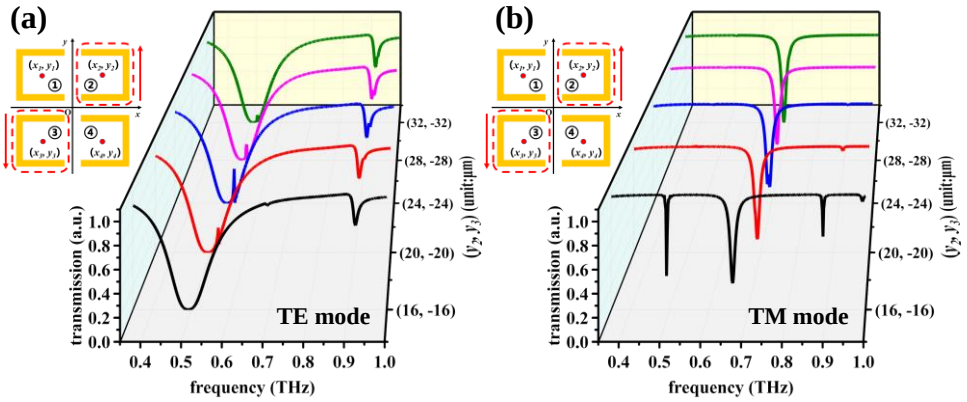

Figure 9. Simulated transmission spectra of RTM device obtained by moving the SRR-2 and SRR-3 meta-atoms along positive and negative y-axis directions in (**a**) TE and (**b**) TM modes, respectively.

4. Conclusions

In conclusion, we present a design of reconfiguring SRR meta-atoms, which exhibits the capability to tune the electromagnetic responses of the incident THz wave by moving SRR meta-atom positions. There are two tuning resonances with a tuning range of 50 GHz in TE mode when SRR-2 and SRR-4 meta-atoms move along positive x-axis direction. On the other hand, there is one single-resonance tuned from 0.67 THz to 0.72 THz in TM mode by moving SRR-1 and SRR-2 meta-atoms along positive y-axis direction. This shows that the resonances can be tuned in a range of several tens of GHz in the situation where the SRR array is still axially symmetric even if the whole configurated pattern is changed. By moving the SRR-2 and SRR-4 meta-atoms along the positive y-axis direction, there is an EIT resonance in TE mode. Furthermore, the resonances can be transformed from dual-band to multi-band in TE mode by moving the SRR-2 meta-atom along positive x-axis direction. When the position of SRR-2 and SRR-3 meta-atoms are moved along x- or y-axis direction, the switching function is transformed from triple-band to single-band in TM mode. This shows that the asymmetric SRR array can change their EIT resonance from single-band, to dual-band and triple-band. This work provides a detailed investigation of the electromagnetic response of a planar SRR array and paves the way for future studies on tunable metamaterials. It can be potentially used in many applications such as wearable electronic devices, tunable filters, active sensors, modulators and so on.

Author Contributions: Conceptualization, Y.L. and Y.-S.L.; methodology, Y.L. and Y.-S.L.; software, Y.L.; validation, Y.L. and Y.-S.L.; formal analysis, Y.L. and Y.-S.L.; investigation, Y.L. and Y.-S.L.; resources, Y.L. and Y.-S.L.; data curation, Y.L. and Y.-S.L.; writing—original draft preparation, Y.L. and Y.-S.L.; writing—review and editing, Y.L. and Y.-S.L.; supervision, Y.-S.L.; project administration, Y.-S.L.; funding acquisition, Y.-S.L. All authors have read and agreed to the published version of the manuscript.

Funding: This research was funded by the financial support from the National Key Research and Development Program of China (2019YFA0705000).

Conflicts of Interest: The authors declare no conflicts of interest.

References

1. Smith, D.R.; Padilla, W.J.; Vier, D.C.; Nemat-Nasser, S.C.; Schultz, S. Composite Medium with Simultaneously Negative Permeability and Permittivity. *Phys. Rev. Lett.* **2000**, *84*, 4184–4187. [CrossRef] [PubMed]
2. Smith, D.R.; Vier, D.C.; Kroll, N.; Schultz, S. Direct calculation of permeability and permittivity for a left-handed metamaterial. *Appl. Phys. Lett.* **2000**, *77*, 2246–2248. [CrossRef]

3. Chen, H.-T.; Padilla, W.J.; Zide, J.M.O.; Gossard, A.C.; Taylor, A.J.; Averitt, R.D. Active terahertz metamaterial devices. *Nature* **2006**, *444*, 597–600. [CrossRef] [PubMed]
4. Lin, Y.-S.; Dai, J.; Zeng, Z.; Yang, B.-R. Metasurface Color Filters Using Aluminum and Lithium Niobate Configurations. *Nanoscale Res. Lett.* **2020**, *15*, 77–78. [CrossRef] [PubMed]
5. Dai, J.; Xu, R.; Lin, Y.S.; Chen, C.H. Tunable electromagnetic characteristics of suspended nanodisk metasurfac. *Opt. Laser Technol.* **2020**, *128*, 106214. [CrossRef]
6. Lin, Y.-S.; Chen, W. A large-area, wide-incident-angle, and polarization-independent plasmonic color filter for glucose sensing. *Opt. Mater.* **2018**, *75*, 739–743. [CrossRef]
7. Zhan, F.; Lin, Y.S. Tunable Multi-Resonance Using Complementary Circular Metamaterial. *Opt. Lett.* **2020**, *45*, 3633–3636. [CrossRef]
8. Zhong, J.; Lin, Y.-S. Electromechanically Rotatable Cross-Shaped Mid-IR Metamaterial. *Crystals* **2020**, *10*, 431. [CrossRef]
9. Wen, Y.; Liang, Z.; Lin, Y.-S.; Chen, C.-H. Active modulation of polarization-sensitive infrared metamaterial. *Opt. Commun.* **2020**, *463*, 125489. [CrossRef]
10. Mo, Y.; Zhong, J.; Lin, Y.-S. Tunable chevron-shaped infrared metamaterial. *Mater. Lett.* **2020**, *263*, 127291. [CrossRef]
11. Liang, Z.; Liu, P.; Lin, Z.; Zhang, X.; Zhang, Z.; Lin, Y.-S. Electromagnetic responses of symmetrical and asymmetrical infrared ellipse-shape metamaterials. *OSA Contin.* **2019**, *2*, 2153–2161. [CrossRef]
12. Lin, Y.-S. Complementary infrared metamaterials for volatile organic solutions sensing. *Mater. Lett.* **2017**, *195*, 55–57. [CrossRef]
13. Xu, Z.; Lin, Z.; Cheng, S.; Lin, Y.-S. Reconfigurable and tunable terahertz wrench-shape metamaterial performing programmable characteristic. *Opt. Lett.* **2019**, *44*, 3944–3947. [CrossRef] [PubMed]
14. Chen, X.; Lin, Y.-S. Polarization-Sensitive Metamaterials with Tunable Multi-Resonance in the Terahertz Frequency Range. *Crystals* **2020**, *10*, 611. [CrossRef]
15. Xu, T.; Lin, Y.-S. Tunable Terahertz Metamaterial Using an Electric Split-Ring Resonator with Polarization-Sensitive Characteristic. *Appl. Sci.* **2020**, *10*, 4660. [CrossRef]
16. Yang, W.; Lin, Y.-S. Tunable metamaterial filter for optical communication in the terahertz frequency range. *Opt. Express* **2020**, *28*, 17620. [CrossRef]
17. Zheng, D.; Hu, X.; Lin, Y.-S.; Chen, C.-H. Tunable multi-resonance of terahertz metamaterial using split-disk resonators. *AIP Adv.* **2020**, *10*, 025108. [CrossRef]
18. Hu, X.; Zheng, D.; Lin, Y.-S. Actively tunable terahertz metamaterial with single-band and dual-band switching characteristic. *Appl. Phys. A* **2020**, *126*, 110. [CrossRef]
19. Ou, H.; Lu, F.; Liao, Y.; Zhu, F.; Lin, Y.-S. Tunable terahertz metamaterial for high-efficiency switch application. *Results Phys.* **2020**, *16*, 102897. [CrossRef]
20. Lin, Z.; Xu, Z.; Liu, P.; Liang, Z.; Lin, Y.-S. Polarization-sensitive terahertz resonator using asymmetrical F-shaped metamaterial. *Opt. Laser Technol.* **2020**, *121*, 105826. [CrossRef]
21. Liu, P.; Liang, Z.; Lin, Z.; Xu, Z.; Xu, R.; Yao, D.; Lin, Y.-S. Actively tunable terahertz chain-link metamaterial with bidirectional polarization-dependent characteristic. *Sci. Rep.* **2019**, *9*, 9917. [CrossRef] [PubMed]
22. Xu, Z.; Lin, Y.-S. A Stretchable Terahertz Parabolic-Shaped Metamaterial. *Adv. Opt. Mater.* **2019**, *7*, 1900379. [CrossRef]
23. Cheng, S.; Xu, Z.; Yao, D.; Zhang, X.; Zhang, Z.; Lin, Y.-S. Electromagnetically induced transparency in terahertz complementary spiral-shape metamaterials. *OSA Contin.* **2019**, *2*, 2137–2144. [CrossRef]
24. Zhang, C.; Cheng, Q.; Yang, J.; Zhao, J.; Cui, T.-J. Broadband metamaterial for optical transparency and microwave absorption. *Appl. Phys. Lett.* **2017**, *110*, 143511. [CrossRef]
25. Liu, P.Q.; Luxmoore, I.; Mikhailov, S.A.; Savostianova, N.A.; Valmorra, F.; Faist, J.; Nash, G.R. Highly tunable hybrid metamaterials employing split-ring resonators strongly coupled to graphene surface plasmons. *Nat. Commun.* **2015**, *6*, 8969. [CrossRef]
26. Jiang, S.-C.; Xiong, X.; Hu, Y.-S.; Hu, Y.-H.; Ma, G.-B.; Peng, R.; Sun, C.; Wang, M. Controlling the Polarization State of Light with a Dispersion-Free Metastructure. *Phys. Rev. X* **2014**, *4*, 021026. [CrossRef]
27. Kenney, M.; Grant, J.P.; Shah, Y.D.; Carranza, I.E.; Humphreys, M.; Cumming, D.R.S. Octave-Spanning Broadband Absorption of Terahertz Light Using Metasurface Fractal-Cross Absorbers. *ACS Photon.* **2017**, *4*, 2604–2612. [CrossRef]

28. Xu, R.; Liu, X.; Lin, Y.-S. Tunable ultra-narrowband terahertz perfect absorber by using metal-insulator-metal microstructures. *Results Phys.* **2019**, *13*, 102176. [CrossRef]
29. Ou, H.; Lu, F.; Xu, Z.; Lin, Y.-S. Terahertz Metamaterial with Multiple Resonances for Biosensing Application. *Nanomaterial* **2020**, *10*, 1038. [CrossRef]
30. Liang, Z.; Wen, Y.; Zhang, Z.; Liang, Z.; Xu, Z.; Lin, Y.-S. Plasmonic metamaterial using metal-insulator-metal nanogratings for high-sensitive refraction index sensor. *Results Phys.* **2019**, *15*, 102602. [CrossRef]
31. Xu, R.; Lin, Y.-S. Characterizations of reconfigurable infrared metamaterial absorbers. *Opt. Lett.* **2018**, *43*, 4783–4786. [CrossRef]
32. Xu, R.; Luo, J.; Sha, J.; Zhong, J.; Xu, Z.; Tong, Y.; Lin, Y.-S. Stretchable IR metamaterial with ultra-narrowband perfect absorption. *Appl. Phys. Lett.* **2018**, *113*, 101907. [CrossRef]
33. Lin, Y.-S.; Huang, C.-Y.; Lee, V.C. Reconfiguration of Resonance Characteristics for Terahertz U-Shape Metamaterial Using MEMS Mechanism. *IEEE J. Sel. Top. Quantum Electron.* **2014**, *21*, 93–99. [CrossRef]
34. Lin, Y.-S.; Liao, S.; Liu, X.; Tong, Y.; Xu, Z.; Xu, R.; Yao, D.; Yu, Y. Tunable terahertz metamaterial by using three-dimensional double split-ring resonators. *Opt. Laser Technol.* **2019**, *112*, 215–221. [CrossRef]
35. Zhang, Z.; Zhang, X.; Liang, Z.; Cheng, S.; Liu, P.; Lin, Y.-S. Reconfigurable double C-shape metamaterial (DCM) for a terahertz resonator. *OSA Contin.* **2019**, *2*, 3026–3036. [CrossRef]
36. Zhang, X.; Lin, Y.-S. Actively electromagnetic modulation of IHI-shaped terahertz metamaterial with high-efficiency switching characteristic. *Results Phys.* **2019**, *15*, 102532. [CrossRef]
37. Lu, F.; Ou, H.; Liao, Y.; Zhu, F.; Lin, Y.-S. Actively switchable terahertz metamaterial. *Results Phys.* **2019**, *15*, 102756. [CrossRef]